Drought and ABA acid effects on aquaporin content translate into changes in hydraulic conductivity and leaf growth rate: A trans-scale approach

Boris Parent, Charles Hachez, Elise Redondo, Thierry T. Simonneau, François Chaumont, Francois F. Tardieu

Drought and Abscisic Acid Effects on Aquaporin Content Translate into Changes in Hydraulic Conductivity and Leaf Growth Rate: A Trans-Scale Approach[1][W][OA]

Boris Parent, Charles Hachez, Elise Redondo, Thierry Simonneau, François Chaumont, and François Tardieu*

INRA, UMR 759 Laboratoire d'Ecophysiologie des Plantes sous Stress Environnementaux, F–34060 Montpellier, France (B.P., T.S., F.T.); Institut des Sciences de la Vie, Université catholique de Louvain, B–1348 Louvain-la-Neuve, Belgium (C.H., F.C.); and Biogemma Auvergne, ZI du Brézet, F–63028, Clermont-Ferrand, France (E.R.)

The effects of abscisic acid (ABA) on aquaporin content, root hydraulic conductivity (Lp_r), whole plant hydraulic conductance, and leaf growth are controversial. We addressed these effects via a combination of experiments at different scales of plant organization and tested their consistency via a model. We analyzed under moderate water deficit a series of transformed maize (*Zea mays*) lines, one sense and three antisense, affected in *NCED* (for 9-cis-epoxycarotenoid dioxygenase) gene expression and that differed in the concentration of ABA in the xylem sap. In roots, the mRNA expression of most aquaporin *PIP* (for plasma membrane intrinsic protein) genes was increased in sense plants and decreased in antisense plants. The same pattern was observed for the protein contents of four PIPs. This resulted in more than 6-fold differences between lines in Lp_r under both hydrostatic and osmotic gradients of water potential. This effect was probably due to differences in aquaporin activity, because it was nearly abolished by a hydrogen peroxide treatment, which blocks the water channel activity of aquaporins. The hydraulic conductance of intact whole plants was affected in the same way when measured either in steady-state conditions or via the rate of recovery of leaf water potential after rewatering. The recoveries of leaf water potential and elongation upon rehydration differed between lines and were accounted for by the experimentally measured Lp_r in a model of water transfer. Overall, these results suggest that ABA has long-lasting effects on plant hydraulic properties via aquaporin activity, which contributes to the maintenance of a favorable plant water status.

During water deficit, abscisic acid (ABA) is involved in three strategies used by plants to avoid deleterious leaf dehydration. First, plants close stomata and decrease transpiration rate, with a consensus on the effect of ABA (Zhang and Davies, 1990a; Borel et al., 2001) but differences regarding its origin in the plant (Christmann et al., 2007; Endo et al., 2008). Second, plants decrease shoot growth in order to limit transpiration. The contribution of ABA to this reduction differs between studies, with either positive effects of ABA (Sharp, 2002; Sansberro et al., 2004; Thompson et al., 2007a) or negative effects (Zhang and Davies, 1990b; Ben Haj Salah and Tardieu, 1997; Bacon et al., 1998). Third, plants tend to control root water uptake and/or plant water status via root growth (Sharp, 2002) and root hydraulic conductivity (Lp_r; Kaldenhoff et al., 2008; Maurel et al., 2008).

The effects of soil water deficit and of ABA on Lp_r are controversial. Water deficit tends to decrease Lp_r (Lo Gullo et al., 1998; Zhang and Tyerman, 1999; North et al., 2004; Vandeleur et al., 2009), while ABA has the opposite effect in most studies (Morillon and Chrispeels, 2001; Thompson et al., 2007a). In a few studies, exogenous ABA had no effect or a negative effect on hydraulic conductivity (Wan and Zwiazek, 1999; Aroca et al., 2003), while in others a positive effect has been observed at both the cell level (Hose et al., 2000; Wan et al., 2004; Lee et al., 2005) and the whole root level (Quintero et al., 1999; Sauter et al., 2002; Schraut et al., 2005). However, these responses were transient (Hose et al., 2000) and were positive or negative depending on the ABA concentration (Beaudette et al., 2007).

Change in aquaporin mRNA and protein contents in response to water deficit and ABA is also a matter of debate (Kaldenhoff et al., 2008). ABA induces transcription factors that regulate the expression of PIP (for plasma membrane intrinsic protein) aquaporins (Kaldenhoff et al., 1996; Shinozaki et al., 1998). However, exogenous ABA affects a larger number of PIP isoforms than water deficit (Jang et al., 2004), suggesting some degree of independence between ABA and drought signal transduction pathways (Mariaux et al., 1998). In addition, increase in *PIP* mRNA expression is

[1] This work was supported by the Agence Nationale de la Recherche Genoplante project Waterless, the Generation Challenge Programme Generation, the Belgian National Fund for Scientific Research, the Inter-University Attraction Pole Programme-Belgian Science Policy, and the Communauté Française de Belgique-Actions de Recherches Concertées.

* Corresponding author; e-mail tardieu@supagro.inra.fr.

The author responsible for distribution of materials integral to the findings presented in this article in accordance with the policy described in the Instructions for Authors (www.plantphysiol.org) is: François Tardieu (tardieu@supagro.inra.fr).

[W] The online version of this article contains Web-only data.

[OA] Open Access articles can be viewed online without a subscription.

www.plantphysiol.org/cgi/doi/10.1104/pp.108.130682

often transient and dependent on ABA concentration (Zhu et al., 2005; Beaudette et al., 2007) and does not necessarily result in an increase in PIP protein content (Morillon and Chrispeels, 2001; Aroca et al., 2006).

Aquaporins play a key role in radial water transport in roots and leaves under both hydrostatic and osmotic gradients (Steudle, 2000; Tyerman et al., 2002; Maurel et al., 2008). The contribution of aquaporin-mediated water transport has been evaluated with inhibitors, namely mercuric salt (Martre et al., 2001), acid load (Tournaire-Roux et al., 2003), and hydrogen peroxide (H_2O_2; Ye and Steudle, 2006; Boursiac et al., 2008). These studies indicate that water transport by aquaporins accounts for 20% to 85% of the overall water transport depending on the species (Wan and Zwiazek, 1999; Barrowclough et al., 2000). Whereas the importance of aquaporins in Lp_r has been demonstrated (Maurel et al., 2008), the resulting effect on overall plant conductance, leaf water potential, and leaf elongation rate is still poorly studied. Experiments using plants with modified aquaporin expression report differences in leaf water potential during the day (Lian et al., 2004) or during rewetting (Martre et al., 2002).

The purpose of this work was to test whether drought and ABA have consistent effects on plant hydraulic properties at different scales of plant organization, namely the abundance of aquaporin transcripts and proteins, the Lp_r under both osmotic and hydrostatic gradients, the whole plant hydraulic conductance evaluated in steadily transpiring plants or upon rehydration, and the recovery of leaf elongation rate upon rehydration. Hence, we performed independent experiments at each scale of organization and then linked these scales with a model that allows the weighing of relative contributions of Lp_r and other possible causes on the whole plant hydraulic behavior.

To this aim, we have used maize (*Zea mays*) lines affected in the expression of the *NCED/VP14* gene encoding the 9-cis-epoxycarotenoid dioxygenase enzyme, previously identified from the *vp14* mutation (Tan et al., 1997). NCED/VP14 catalyzes the first specific step in ABA biosynthesis and affects ABA production when overexpressed (Thompson et al., 2000, 2007b) or underexpressed (Voisin et al., 2006). *NCED/VP14* expression as well as NCED/VP14 protein content are indeed strongly correlated with ABA levels (Qin and Zeevaart, 1999). These lines were subjected to changes in soil water content, evaporative demand, or pressure on the root system, thereby affecting independently water deficit and the concentration of ABA in the xylem sap.

RESULTS

A Set of Maize Lines Transformed on the *NCED/VP14* Gene Differed in $[ABA]_{xyl}$, Stomatal Conductance, and Transpiration Rate in Greenhouse Experiments

The genetic transformation was targeted to one NCED gene with sense and antisense constructs. It resulted in three antisense lines (AS1, AS2, and AS5) and one sense line (S). The concentrations of ABA in the xylem sap ($[ABA]_{xyl}$) differed significantly between AS, null transformants, and S plants in well-watered conditions as well as in moderate water deficit (Fig. 1A), consistent with the lower and higher transcript amounts of *NCED/VP14* in AS and S plants, respectively (Supplemental Fig. S1). Null transformants resulting from each transformation event had insignificant differences in $[ABA]_{xyl}$. Therefore, they were pooled in all figures and are referred to as WT hereafter. Plants of the three AS lines had a low but still appreciable $[ABA]_{xyl}$ in both well-watered and dry

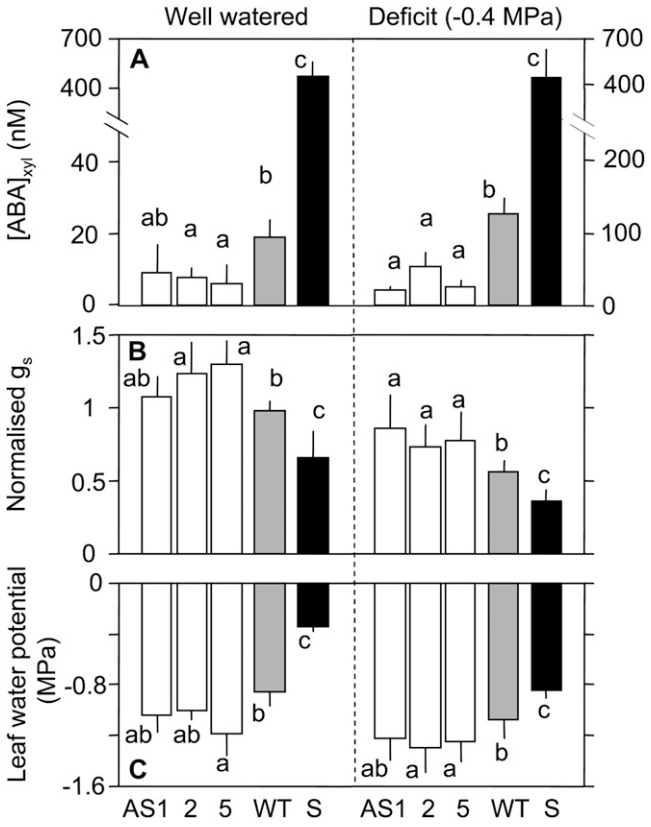

Figure 1. ABA concentration in the xylem sap (A), midday stomatal conductance (B; g_s), and leaf water potential (C) in three greenhouse experiments with high evaporative demand (experiments 1–3 in Table II; only days with noontime VPDs from 2 to 2.8 kPa were kept in the analysis). Two contrasting water regimes were compared, well watered and a mild water deficit with a soil water potential of −0.4 MPa, for three AS lines, one S line, and their null transformants (pooled and named WT). A, Xylem sap was collected at the end of the night. B, Stomatal conductance was measured at noon. Because g_s of WT plants differed between experiments, from 120 to 180 mmol m^{-2} s^{-1}, it was normalized by the mean value in WT. C, Leaf water potential was measured at noon in nonexpanding leaves. Data were averaged from the three experiments ($n > 10$ in each condition and line). Error bars indicate confidence intervals at the 0.95 risk level. Bars associated with the same letter indicate nonsignificant differences ($P > 0.05$) in a Benjamini and Hochberg *t* test (Benjamini and Hochberg, 1995).

conditions (Fig. 1A; insignificant differences between AS lines), so their stomata closed under water deficit (Fig. 1B). The transpiration flow measured at midday in moderately droughted plants grown in the greenhouse was significantly higher in the three AS plants than in WT plants (Fig. 2A). Sense plants had the opposite behavior, with a high $[ABA]_{xyl}$ (>400 nM), a low stomatal conductance in both well-watered and droughted plants (Fig. 1, A and B), and a transpiration rate per unit leaf area 2-fold lower than that of WT plants (Fig. 2A). AS plants had comparable phenotypes to WT plants, except that they germinated more quickly and wilted slightly earlier upon water shortage. Because the three AS lines had similar behaviors, most studies were carried out in the AS5 line. S plants had a smaller leaf area than AS and WT plants, due to differences in leaf growth rate in well-watered conditions before the experiment.

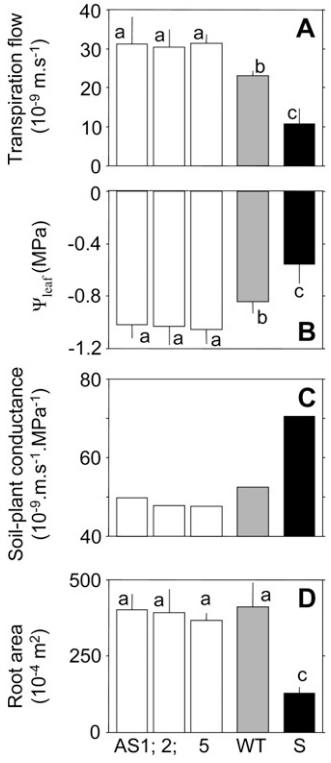

Figure 2. Transpiration flow (A), leaf water potential (B; Ψ_{leaf}), calculated conductance of water transfer from soil to leaves (C), and root area (D) in a greenhouse experiment with moderate evaporative demand (experiment 3 in Table II; only days with noontime VPD from 1.3 to 1.8 kPa were kept in the analysis) and water deficit (soil water potential of −0.4 MPa). Three AS lines (AS1, AS2, and AS5) and one S line were compared with null transformants (WT). A and B, Transpiration flow and leaf water potential were measured at noontime (n = 4–10). C, Soil-leaf resistance was calculated as the ratio of the difference of potential between soil and leaves to the transpiration flow. D, Root area of three plants of each line at the six-leaf stage. Bars represent mean values (n = 3–8). Error bars indicate confidence intervals at the 0.95 risk level. Bars associated with the same letter indicate nonsignificant differences ($P > 0.05$) in a Benjamini and Hochberg t test (Benjamini and Hochberg, 1995).

PIP Expression in Roots Was Highly Dependent on ABA Biosynthesis

We compared by quantitative reverse transcription (RT)-PCR the expression levels of *ZmPIP* genes in roots of S, WT, and AS plants (Fig. 3). Plants were grown hydroponically and sampled in the early morning at the same phenological stage and root water potential (72-h polyethylene glycol [PEG] stress, −0.4 MPa) as in the water deficit treatments presented in Figures 1 and 2. Expression levels of the five *PIP* genes belonging to the PIP1 subgroup were significantly higher in S plants and lower in AS plants. The strongest effect was observed for *ZmPIP1;2*, *ZmPIP1;3*, and *ZmPIP1;4*, with a 9- to 10-fold difference in expression between AS and S plants ($P < 10^{-5}$). In the *PIP2* subgroup, the expression levels of two *PIP* genes were increased in S plants (*ZmPIP2;1* and *ZmPIP2;2*) and those of four *PIP* genes were decreased in AS plants (*ZmPIP2;1*, *ZmPIP2;2*, *ZmPIP2;3*, and *ZmPIP2;6*). Overall, for most *PIP* isoforms, the expression levels were affected by changes in ABA biosynthesis in a long-lasting way, with higher expression levels in S plants and lower levels in AS plants.

Increased and Decreased ABA Biosynthesis Largely Affected the Protein Contents of Three PIPs in Roots and of Two PIPs in Leaves

PIPs belonging to either PIP1 or PIP2 subgroups were chosen for further investigation using specific antibodies raised against each PIP (Fig. 4A). These were ZmPIP1;2, whose gene expression was the most increased in S plants and four proteins of the PIP2 subgroup; and ZmPIP2;1/2;2, ZmPIP2;5, and ZmPIP2;6, whose gene expression was the highest in maize roots in this study and in the study of Hachez et al. (2006). All ZmPIP immunoblot analyses revealed two major bands at about 28 and 55 kD, corresponding to monomeric and dimeric forms (Fig. 4A). Primary roots coming from AS lines showed strongly decreased amounts of the isoforms ZmPIP1;2 (−75%), ZmPIP2;1/2;2 (−43%), and ZmPIP2;5 (−49%; Fig. 4). Opposite effects on the amounts of the same proteins were observed in the S line, especially in ZmPIP1;2 (12-fold increase; Fig. 4). The intermediate band (around 40 kD) detected with ZmPIP2;6 antibodies corresponds to a cross-reacting unrelated protein (data not shown).

Leaves also showed differences in PIP protein amounts, although to a lesser extent than roots (Fig. 4B). S plants had higher amounts of ZmPIP1;2 and ZmPIP2;1/2;2 than WT plants (1.9- and 1.3-fold increases, respectively), with an opposite effect for AS plants (0.75 and 0.9). In contrast, no signals were

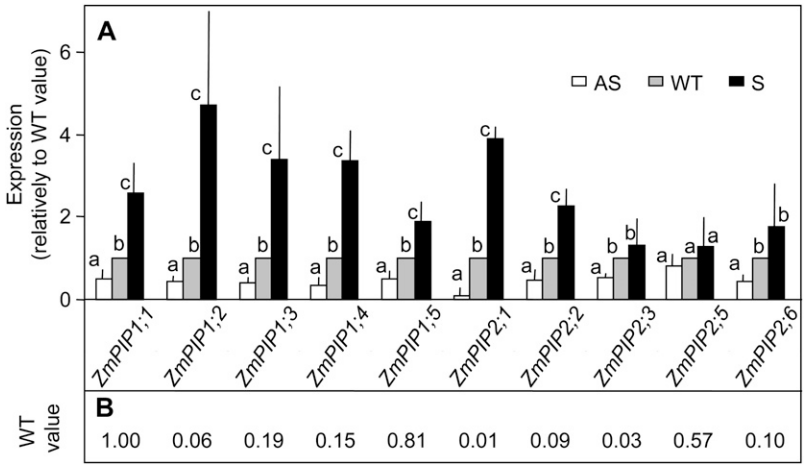

Figure 3. Expression levels (measured by quantitative RT-PCR) of 10 *ZmPIP* genes in roots. Plants were grown hydroponically (experiment 7 in Table II) and sampled at the same phenological stage as in Figures 1 and 2. The geometric mean of the expression levels of two control genes (tubulin and actin) was used to normalize data. Expression levels of *ZmPIP1;6* and *ZmPIP2;4* were very low (<10- to 4-fold the *ZmPIP1;1* level) and are not shown. A, Expression levels in AS (AS5) and S plants relative to expression in WT plants. Bars represent mean values ($n = 6$). Error bars indicate confidence intervals at the 0.95 risk level. Bars associated with the same letter indicate nonsignificant differences ($P > 0.05$) in a t test comparing each normalized value with unity. B, Expression level in WT plants, with PIP1;1 as a reference.

detected for ZmPIP2;5 and ZmPIP2;6, which were shown to be much less expressed in leaves compared with roots (Hachez et al., 2008).

Increased and Decreased ABA Biosyntheses Affected the Lp_r in Hydroponics, But This Effect Was Abolished by H_2O_2 Treatment

Root systems were placed during the morning in a hydroponic solution, with a hydrostatic tension of −0.02 MPa applied to the hypocotyls of detopped plants. WT plants released a stable water flux for 40 min, which was multiplied by 3 and 0.5 in S and AS plants, respectively (Fig. 5A). H_2O_2 was then brought to the nutrient solution in order to decrease the hydraulic conductivity of the transcellular pathway (Ye and Steudle, 2006; Boursiac et al., 2008). This caused a steep decrease in water flux in both S and WT plants but had nearly no effect in AS plants. The water fluxes, therefore, were insignificantly different in the three treatments after the H_2O_2 treatment.

Differences in water flux were analyzed by measuring root hydraulic conductivities under hydrostatic (Lp_h) and osmotic (Lp_{os}) gradients of water potential. Lp_h was calculated as the slope of the relationship between the applied suction and the flux released by

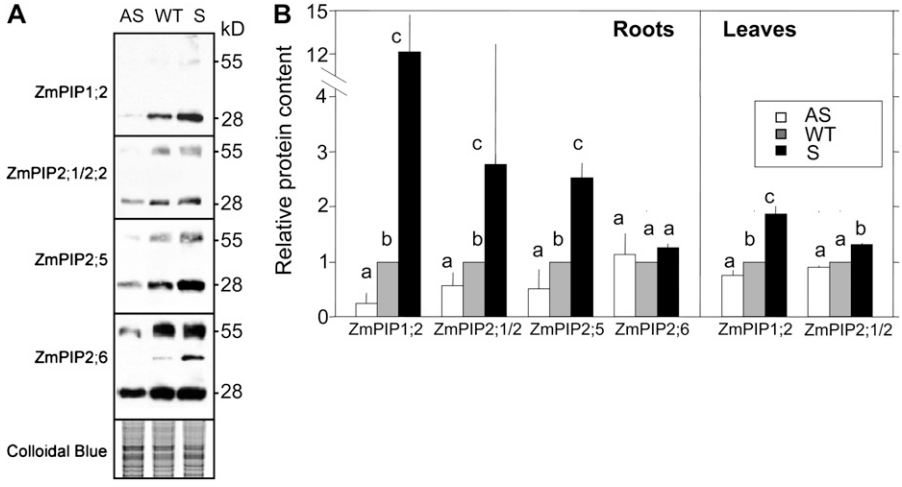

Figure 4. Immunoblots of ZmPIPs and protein quantification in AS (AS5), WT, and S plants. Plants were grown and sampled in the same conditions as in Figure 3 (experiment 5 in Table II). A, Western blot on root protein extract. Microsomal membranes were extracted from the first 5 cm of primary roots of plants grown hydroponically until the six-leaf stage and then subjected to 3 d at −0.4 MPa obtained with the addition of PEG to the solution. The proteins (15 μg) were subjected to western blotting using antibodies against plasma membrane ATPase (H^+-ATPases), ZmPIP1;2, ZmPIP2;1/2;2, ZmPIP2;5, and ZmPIP2;6. Colloidal blue gel staining was used as a gel-loading control. B, Quantification of PIP protein spots in roots and mature leaves coming from two independent experiments (three WT, two AS, and one S plant in each experiment). Three blot exposure times were used for the quantification. Each data point is a mean value of three experiments relative to the intensity in WT plants. Error bars indicate confidence intervals at the 0.95 risk level. Bars associated with the same letter indicate nonsignificant differences ($P > 0.05$) in a Benjamini and Hochberg t test (Benjamini and Hochberg, 1995).

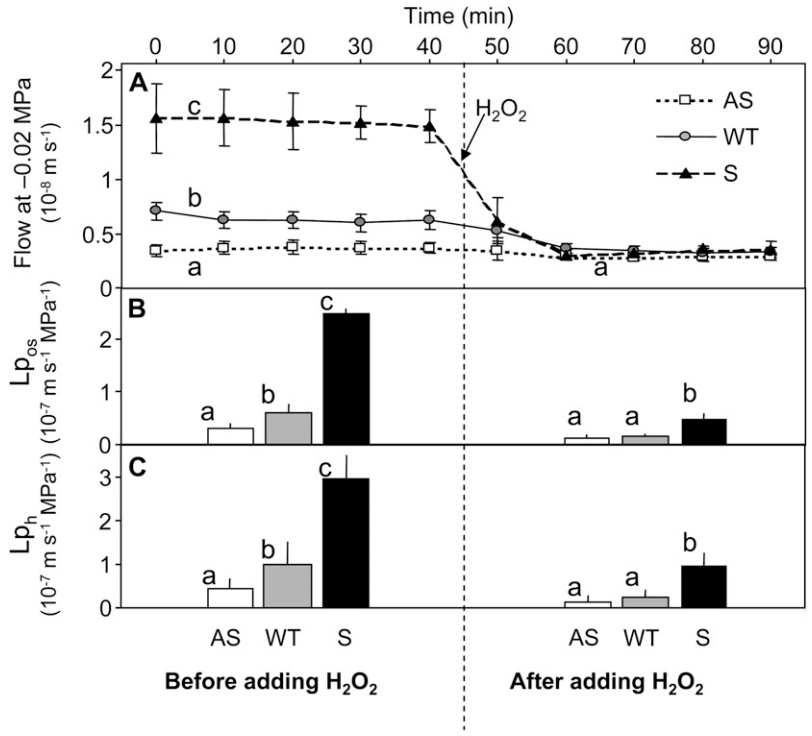

Figure 5. Water flow (A) through excised root systems placed in a nutrient solution and subjected to a tension of −0.02 MPa, and Lp_r under osmotic (B; Lp_{os}) and hydrostatic (C; Lp_h) gradients, before and after the addition of H_2O_2 in the nutrient solution, in AS (AS5), null transformants (WT), and S plants. Plants were grown in the same conditions as in Figures 3 and 4 (experiments 6 and 7 in Table II). A, Mean values of water flow (n = 3–10). The nutrient solution was changed to 2 mM H_2O_2 at 40 min. B, Lp_{os} was calculated from free exudation flow and osmotic gradient between the solution and the xylem sap (n = 4–9). C, Lp_h was calculated as the slope of water flow under a hydrostatic gradient (0, −0.02, −0.04, and −0.06 MPa; n = 4–9). Error bars indicate confidence intervals at the 0.95 risk level. Bars or lines associated with the same letter indicate nonsignificant differences ($P > 0.05$) in a Benjamini and Hochberg t test (Benjamini and Hochberg, 1995).

the root system at −0.02, −0.04, and −0.06 MPa. Lp_{os} was calculated as the ratio between the free exudation flux and the gradient of osmotic potential between the nutrient solution and the sap released by the root system. Both Lp_h and Lp_{os} were highly affected by the manipulation of ABA synthesis before the H_2O_2 treatment (Fig. 5, B and C). AS plants had a lower Lp_h and Lp_{os} (−45% and −52%, respectively) than WT plants, while the S plants had higher Lp_h and Lp_{os} (3- and 4-fold, respectively). Differences in Lp_h and Lp_{os} between AS and WT plants were abolished after the H_2O_2 treatment, and those between S and WT plants were strongly reduced. The fact that flows were similar between WT and S plants after H_2O_2 treatment despite differences of Lp_r was due to a lower gradient of osmotic potential between the solution and the xylem sap in S plants.

Overall, these results show that the manipulation of ABA synthesis strongly affected the water flux through the root system via changes in the hydraulic conductivities under both hydraulic and osmotic gradients. This effect was strongly reduced or disappeared with the H_2O_2 treatment, with a drop in Lp_r that can be interpreted as the contribution of aquaporins to the water flux.

The Total Hydraulic Conductance between Soil and Leaves Increased with ABA Biosynthesis

The total hydraulic conductance between soil and leaves was estimated in a greenhouse experiment by dividing the water flux by the gradient of water potential between soil and leaves (Fig. 2C). Leaf water potential of AS plants was lower than that of WT plants in well-watered conditions as well as in water deficit (Fig. 2B; see also Fig. 1C), while transpiration rate was higher in AS than in WT plants (Fig. 2A). Sense plants had a significantly higher leaf water potential in all conditions, consistent with a lower transpiration rate. The three AS lines had lower hydraulic conductances, and the S line had a higher conductance than the WT plants (Fig. 2C). The differences in soil-plant conductance were not due to changes in root system architecture, because root length and area were very close in WT and AS plants and were lower in S plants than in WT plants (Fig. 2D). Hence, the higher hydraulic conductance observed in S plants in spite of a lower root area suggests a high Lp_r.

S and AS Lines Exhibited Marked Differences in Leaf Rehydration Half-Times and Recovery of Leaf Elongation Rate

We have evaluated the consequences of observed differences in Lp_r on the time courses of the recoveries of leaf water status and leaf elongation rate upon rehydration in a growth chamber experiment with soil-grown plants. Plants initially subjected to a soil water potential of −0.4 MPa and a vapor pressure deficit (VPD) of 2.5 kPa were rewatered and subjected to dark conditions at a VPD of 0.8 kPa that virtually stopped transpiration (time 0; Fig. 6). Before rewatering, leaf water potential differed between lines, consistent with experiments in

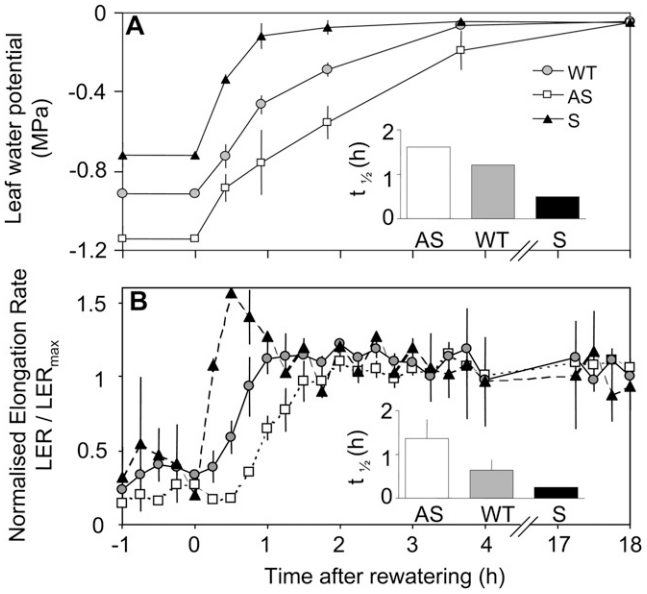

Figure 6. Time courses of recoveries of leaf water potential (A) and of leaf elongation rate (LER; B) upon rewatering in AS (AS5), WT, and S plants in a growth chamber experiment (experiment 3 in Table II; n = 3–10). Normalized leaf elongation rates were calculated as the absolute leaf elongation rate divided by the mean rate observed in the same line during the night in well-watered plants. Plants were transpiring under high evaporative demand (VPD = 2.5 kPa) and subjected to water deficit (soil water potential, −0.4 MPa) until time 0 h. At that time, plants were rewatered and lights were turned off. Insets show half-times ($t_{1/2}$) of recovery. Error bars indicate confidence intervals at the 0.95 risk level.

the greenhouse (Figs. 1 and 2), with higher and lower values in S and AS plants, respectively, than in WT plants. Leaf elongation rates normalized by their maximum values under well-watered conditions for each line also differed before rewatering, with highest and lowest values for S and AS plants, respectively.

Leaf water potential recovered more rapidly in S plants and more slowly in AS plants compared with WT plants, with half-times of 0.5, 1.2, and 1.6 h, respectively (Fig. 6B, inset). Full recovery of leaf water potential occurred in 3, 5, and 7 h, respectively, and all lines reached a common water potential after 18 h. The recovery of leaf elongation rate also largely differed between the three lines, with the same trend as that of leaf water potential. It was more rapid than the recovery of leaf water potential, with half-times and times for full recovery of about 50% of those corresponding to leaf water potential. This difference in time course of recovery was consistently observed in three experiments in the growth chamber (data not shown).

The Differences in Time Course of Rehydration between Lines Are Accounted for by a Model Taking into Account the Measured Hydraulic Parameters

We have evaluated the relative contributions of Lp_r and other possible causes of the differences in time courses presented in Figure 6, with the sensitivity analysis of a model. The model of stomatal control, biosynthesis of ABA, and water transfer is that of Tardieu and Davies (1993), widely tested since then and used by other groups (Dewar, 2002; Gutschick and Simonneau, 2002). It was combined with a model that calculates the water potential at leaf evaporating sites and with a module of capacitance, which allows the calculation of recovery rates (see ''Materials and Methods''). The parameters used in the model are presented in Table I, and the outputs are presented in Figure 7 for S, WT, and AS plants.

In transpiring plants (before time 0), leaf and xylem water potentials of simulated plants were lower in AS plants than in WT and S plants, because of a higher stomatal conductance that caused a higher water flux,

Table I. *Plant characteristics in the three treatments and parameters of the model of water transfer*

All parameters are as described by Tardieu and Davies (1993) with values for maize, except those in this table. ABA synthesis, ABA = $\alpha + \beta\,\psi_{root}$, where α is the ABA synthesis at a water potential of 0 and β is the increase in ABA synthesis with root water potential (ψ_{root}). Hydraulic conductivities and conductances are as in the text. The parameters of the pressure-volume curves are as described in ''Materials and Methods.''

Characteristic	Unit	AS	WT	S	Origin
ABA synthesis, constitutive, α	μmol m^{-3}	0	0	400	Fitted from Figure 1 and data at other water potentials
ABA synthesis, response to root water potential, β	μmol m^{-3} MPa^{-1}	−600	−600	−50	Fitted from Figure 1 and data at other water potentials
Root hydraulic conductivity, Lp_r	m s^{-1} MPa^{-1} 10^{-7}	0.421	0.971	2.92	Measured (Fig. 5)
Conductance from xylem to evaporating sites, g_{x-s} (Eq. 3)	mg MPa^{-1} s^{-1} plant^{-1}	7	7	7	Measured
Conductance from xylem to leaf cells, g_{x-l} (Eq. 4)	mg MPa^{-1} s^{-1} plant^{-1}	0.40	0.40	0.40	Fitted on rehydration data
Pressure-volume parameter, n (Eq. 7)		1.6	1.6	1.6	Parameters of measured pressure-volume curve (Fig. 8)
Pressure-volume parameter, α (Eq. 7)		0.075	0.075	0.075	Parameters of measured pressure-volume curve (Fig. 8)
Root area	cm^2	350	350	150	Measured (Fig. 2)
Leaf area	cm^2	110	110	55	Measured
Plant volume	mm^3	9,000	9,000	4,500	Estimated from leaf area

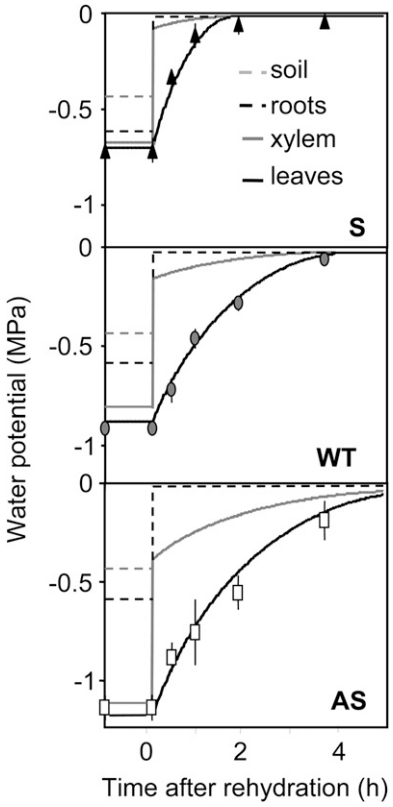

Figure 7. Simulated time course of recovery of water potential in the soil, roots, xylem, and leaves in AS, WT, and S plants. Symbols represent experimental measurements of leaf water potential.

consistent with experimental data. Both this steady state and the recovery of leaf water potential after rehydration could be adequately simulated by the model without the necessity of additional parameters. In particular, a single value for the hydraulic conductance of leaf tissues ($g_{x\text{-}l}$) could be assumed for the WT, AS, and S lines. The model was then used to determine the contributions of several possible causes for the differences in time courses of leaf rehydration. (1) The elastic modulus had here a minor role because all studied lines had similar pressure-volume curves (Fig. 8). (2) The hydraulic conductance of the path between the xylem and leaf cells ($g_{x\text{-}l}$) could potentially have an important effect on the recovery of water potential according to the model. However, simulations with measured values of Lp_r accounted for the whole differences between AS, WT, and S lines, leaving a marginal role or no role for differences in $g_{x\text{-}l}$. This is consistent with the low differences in PIP amounts in leaves. Simulations were only slightly improved if a small difference in $g_{x\text{-}l}$ was assumed between lines, but the effect was too small to justify different fitted values of $g_{x\text{-}l}$ between lines (Table I). (3) The volume of water in the leaf tissues potentially has a large effect on the time courses of leaf water potential upon rehydration. It did not contribute to the difference between AS and WT plants, which had similar leaf areas and weights, but accounted for a large part of the difference between WT and S plants. When simulations were run with a common leaf water volume, the time course of rehydration still differed between WT and S plants, but with a half-time in S plants that increased to 1 h versus 0.5 h in experimental data (Fig. 9).

Overall, this sensitivity analysis suggests that the Lp_r measured in detached root systems accounted for a large part of the differences between lines in whole plant conductance, both in steady-state transpiration and during rehydration. In AS plants, which presented no difference in leaf volume, the increase in half-time of rehydration could be entirely attributed to differences in Lp_r. Part of the difference between S and WT plants was due to a difference in leaf volume, but Lp_r still accounted for 23% of the difference in half-time of rehydration.

DISCUSSION

Consistent effects were observed across different scales of plant organization, suggesting a simpler picture for the role of ABA on plant hydraulic properties than that presented in the introduction. This was probably because differences in ABA supply to the shoot were stable over a long period, thereby avoiding the complexity of transient effects of exogenous ABA application (Hose et al., 2000; Zhu et al., 2005), and because the effects of ABA and drought were not confused.

Effects of Overproduction or Underproduction of ABA on Aquaporin Gene Expression and Protein Content

ABA increased gene expression and protein content of most PIP isoforms and never decreased them. This is consistent with the results of Jang et al. (2004) obtained in roots of Arabidopsis (*Arabidopsis thaliana*), in which exogenous ABA increased the expression of 12 *PIPs*, although one isoform was decreased by the same treatment. However, this is the first time, to our knowledge, that a long-lasting effect was observed, with a stable increase in expression levels for most *PIPs*, in opposition to the results of Zhu et al. (2005) in maize roots, in which an application of exogenous

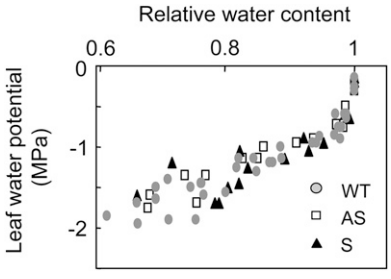

Figure 8. Relationship between leaf relative water content and leaf water potential in AS (AS5), WT, and S plants (experiment 4 in Table II). Each point shows one coupled value of relative water content and water potential corresponding to one leaf.

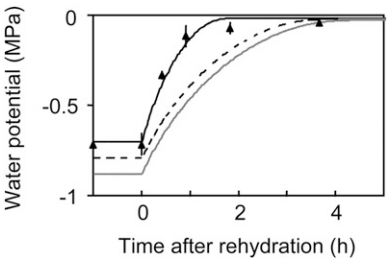

Figure 9. Sensitivity analysis of several possible causes of the difference in time courses between WT and S lines. Simulations were carried out taking into account differences in root hydraulic conductance only (dashed black line) or both hydraulic conductance and leaf volume (black line). The gray line represents WT plants.

ABA caused an increase in expression of only one PIP (*ZmPIP1;2*) after 24 h. This difference is probably due to the fact that changes in ABA concentration were obtained through a transgenic approach in this study instead of the application of exogenous ABA.

The ABA effects on PIP expression resulted in differences between lines in PIP protein contents, in opposition to the data obtained by Morillon and Chrispeels (2001) in Arabidopsis leaves. However, we observed some discrepancies between mRNA and protein levels. ZmPIP2;6 did not show any significant variation at the protein level, although its mRNA expression profile was strongly correlated with endogenous ABA concentration. On the contrary, ZmPIP2;5 was found to have a fairly similar mRNA expression level in the different lines, whereas its protein level showed a clear correlation with ABA content. These observations suggest the existence of posttranscriptional mechanisms to regulate the amount of PIP proteins.

PIP1 gene expression was more affected than that of *PIP2* in our study, especially that of *ZmPIP1;2*, resulting in protein content more affected in ZmPIP1;2 than in PIP2s. This is important in view of the regulating role of this PIP (Zelazny et al., 2007). Gene expression of the PIP2 subfamily was lower than that observed by Hachez et al. (2006) without osmotic or water stress. This could be due to genotypic differences but also to an ABA-independent negative effect of drought on *PIP2* expression, due to mild water stress (Jang et al., 2004).

ABA Effect on Hydraulic Conductivity via Aquaporin Activity Modulation

The variation in the amount of ZmPIP isoforms in AS, WT, and S lines was correlated with the measured differences in Lp_r, indicating that PIP aquaporins play a crucial role in controlling Lp_r. ZmPIP2;1/2;2 and ZmPIP2;5 proteins were reported to be highly expressed in the exodermis and the endodermis, suggesting that they are involved in root radial water movement (Hachez et al., 2006). In addition, the detection of a polar localization of ZmPIP2;5 to the external periclinal side of epidermal cells indicates an important role in water transfer from the soil into the roots (Hachez et al., 2006). The increase in ZmPIP1;2 amount could also induce an increase in the water permeability of root cells. Although PIP1 proteins expressed alone in maize protoplasts were retained in the endoplasmic reticulum, their coexpression with PIP2s resulted in a relocalization to the plasma membrane due to physical interaction (Zelazny et al., 2007). When coexpressed in oocytes, this interaction enhanced the water membrane permeability (Chaumont et al., 2000; Fetter et al., 2004).

The fact that differences in Lp_r disappeared or were largely decreased after H_2O_2 treatment suggests that they were due to differences in aquaporin activity. Boursiac et al. (2008) showed that millimolar concentrations of H_2O_2, as applied in this work, enhance the accumulation of PIPs in intracellular structures, resulting in 60% inhibition of Lp_r. This difference in activity between lines was probably due, at least in part, to the difference in the amount of PIP isoforms in both AS and S plants. We do not rule out the possibility that ABA also had an effect on aquaporin gating, which is the most likely mechanism in short-term experiments with artificial ABA (Hose et al., 2000). However, the latter effect disappeared after 3 h in that study (Hose et al., 2000), suggesting that the effect of ABA on Lp_r, initially due to aquaporin gating, is linked to other mechanisms, including change in PIP content over

Table II. *Summary of experiments carried out in this study*

T_{min} and T_{max}, Minimum and maximum daily temperature during the experiment; VPD_{max}, maximum vapor pressure deficit.

Experiment	Lines	Place	Medium	T_{min}/T_{max}	VPD_{max}	PPFD	Measured Variable
				°C	kPa	$\mu mol\ m^{-2}\ s^{-1}$	
1	AS1, AS2, AS5, WT	Greenhouse	Soil	19/26	2.5	500	g_s, [ABA], ψ
2	AS1, AS2, AS5, WT	Greenhouse	Soil	19/30	3	700	g_s, [ABA], ψ
3	AS1, AS2, AS5, WT, S	Greenhouse	Soil	21/29	2.8	660	g_s, [ABA], ψ, transpiration, root and leaf area
3	AS1, AS2, AS5, WT, S	Growth chamber	Soil	28/28	2.8	400	ψ and leaf elongation rate during rehydration
4–8	AS5, WT, S	Growth chamber	Hydroponics	20/24	0.8	400	Aquaporin expression and protein content, pressure-volume, Lp_r

longer time scales. Therefore, the difference between the clear effect of ABA on Lp_r observed here and the transient (Hose et al., 2000) or nonexisting (Wan and Zwiazek, 2001; Aroca et al., 2003) effects observed by other authors may be due to the difference in mechanisms between endogenous ABA and artificially fed ABA or to a rapid degradation of exogenously applied ABA.

Differences in Lp_r Translate into Changes in Whole Plant Hydraulic Conductance

Two independent ways of evaluating whole plant hydraulic conductance, each of which has its drawbacks, gave consistent results. (1) The conductance calculated from the water flux and the gradient of water potential in the soil-leaves continuum differed between lines. It represents the overall water transport in plants and in the soil and can be affected by any difference in soil water potential (which has a large effect on soil hydraulic conductivity) or in root system architecture (which affects the distance that water has to cross from the soil to the nearest root). This was probably not the case here, because the soil water content did not differ between pots carrying plants of each line and because measured root areas were similar in AS and WT plants and lower in S plants. (2) The difference in the time course of leaf water potential upon rehydration also indicates a difference in overall plant conductance, although other differences between genotypes could also account for this effect. The model showed that the differences in Lp_r measured in detached root systems were sufficient to account for the longer half-time of recovery of leaf water potential in AS plants. The shorter half-time of recovery observed in S plants was only partly due to measured differences in Lp_r, with a contribution of the leaf volume to the behavior of S plants.

Leaf Elongation Rate followed the Changes in Hydraulic Properties upon Rehydration

The effect of ABA on leaf growth via changes in aquaporin activity and Lp_r is usually obscured by the superposition of several effects of ABA at different time scales. In particular, leaf elongation rate during the night was faster and slower, respectively, in AS and S plants than in WT plants in both well-watered and water deficit treatments. This suggests an intrinsic negative effect of ABA on leaf elongation rate consistent with earlier results (Zhang and Davies, 1990b; Ben Haj Salah and Tardieu, 1997; Bacon et al., 1998) and caused a smaller plant size of S plants. During the day, a lower stomatal conductance and higher hydraulic conductivity in S plants compared with WT and AS plants translated into a higher leaf water potential and a higher leaf elongation rate normalized by its value in well-watered plants, as shown in Figure 6.

The complex situation described above led us to concentrate this study on the changes in leaf elongation rate during rehydration. The first surprising result was that growth recovery after rehydration had half-times of around 1 h. The recovery of leaf elongation rate was even faster than that of leaf water potential and responded to ABA production with half-times lower for the S line and higher for the AS line than for WT plants. The beneficial effect of ABA on Lp_r, therefore, had consequences on leaf water status and then on leaf elongation rate upon rewatering.

MATERIALS AND METHODS

Genetic Material

A series of transformed maize (*Zea mays*) lines were analyzed, one S line (S) and three AS lines (AS1, AS2, and AS5; already presented in the study of Voisin et al. [2006] with the names FCN-001a, FCN-002a, and FCN-005b, respectively). AS lines were engineered by transformation of the line A188 with *Agrobacterium tumefaciens* carrying the pRec518 superbinary vector (Ishida et al., 1996). The pRec518 vector was obtained after recombination between *A. tumefaciens* pSB1 superbinary vector and pBIOS518, which contains a 1.8-kb coding sequence of NCED/VP14 under the constitutive viral promoter *Cassava vein mosaic virus* (CsVMV) and the upstream Nos terminator. pBIOS518 carries the BAR marker gene driven by the actin constitutive promoter and its first intron and is stopped by the Nos terminator. The sense transgenic line, FVC-002b (S), was engineered by biolistic and was obtained by cotransformation of the pCsVMVNCEDsens plasmid, which carries the NCED/VP14 sequence in the sense orientation under the CsVMV constitutive promoter and upstream Nos terminator, and the pDM302 vector, which contains the following cassette: actin promoter and its first intron, marker gene BAR, and the Nos terminator (Gordon-Kamm et al., 1990). Primary transformants were grown in vitro, acclimated in the greenhouse (16-h day, 24°C, 80% relative humidity and 8-h night, 20°C, 100% relative humidity). They were then crossed with the line A188, and the resulting material (T1) was used in this study. It was checked by Southern blotting that transformed plants containing one or two copies of the transgene. To identify T1 plants carrying the insertion (50% of the plants), a PCR test (Taq Hot Start master mix; Qiagen) was performed in each studied plant on a 50-mg fresh weight leaf sample at the third leaf stage. Primers were designed for the *NCED/VP14* gene (forward, 5′-AGTTGTTGTCACCCAGTCCAG-3′; reverse, 5′-CACGCACCGATAGCCACA-3′). In all cases, nontransformed plants, sisters from transformed plants, were used as controls.

Plant Growth Conditions in Hydroponics

Maize seeds were placed in tubes with a wet sponge and germinated at 24°C in the dark and saturated air. After 3 to 5 d, the germinated seeds were placed in the growth chamber with their roots bathing in a continuously aerated solution with the following composition: 0.25 mM $CaSO_4$, 0.8 mM KNO_3, 0.6 mM KH_2PO_4, 0.2 mM $MgSO_4(7H_2O)$, 0.4 mM NH_4NO_3, 2×10^{-3} mM $MnSO_4$, 0.4×10^{-3} mM $ZnSO_4$, 0.4×10^{-3} mM $CuSO_4$, 0.2×10^{-3} mM Na_2MoO_4 $(2H_2O)$, 1.6×10^{-2} mM H_3Bo_3, 0.04 mM Fe-EDDHA, and 2.5 mM MES, pH 5.5 to 5.8. The hydroponic solution was renewed every third to fourth day. Air temperature and relative humidity were measured at plant level every 30 s with two sensors (HMP35A; Vaisala Oy). The temperature of the meristematic zone was measured with fine copper-constantan thermocouples (0.2 mm diameter), inserted between the sheaths of leaves 2 and 3 of four to six plants per experiment. Photosynthetic photon flux density (PPFD) was measured every 30 s using two sensors (LI-190SB from Li-Cor and SOLEMS 01/012/012). All climatic data were averaged and stored every 15 min in a data logger (Campbell Scientific, LTD-CR10X Wiring Panel). Environmental conditions are summarized in Table II.

Plant Growth Conditions in the Greenhouse

Plants were grown in PVC columns (0.23 m diameter and 0.4 m height) containing a 40:60 (v/v) mixture of filtered loamy soil (particle diameter ranging from 0.1 to 4 mm) and organic compost. Columns were filled with 10.5 kg of soil and sampled for measurement of water content at filling time. Seeds were sown at 2.5 cm depth and watered with water until the two-leaf stage

and with a modified one-tenth-strength Hoagland solution after that. Environmental data were measured as above and are presented in Table II (experiments 1–3).

Soil water content was determined by weighing columns automatically every 15 min. Differences in weight were attributed to changes in soil water content, after correction for the increase in mean plant biomass as a function of phenological stage and for the effect of displacement transducers. A water-release curve of the soil was obtained by measuring the soil water potential of soil samples with different water contents, in the range 0.4 to 0.2 g g^{-1} (WP4-T Dewpoint Meters; Decagon Devices), thereby allowing calculation of the mean soil water potential in each soil column every 15 min.

Plant Growth Conditions in the Growth Chamber, Rewetting Experiment, and Measurement of Leaf Elongation Rate

Plants with mild water deficit (soil water potential of −0.4 MPa) and growing in the greenhouse under high evaporative demand were transferred at noontime to a growth chamber with a moderate evaporative demand (Table II, experiment 3; VPD = 2.5 kPa, 28°C, PPFD = 400 μmol m^{-2} s^{-1}). They were left to transpire under these conditions for 3 h, during which leaf water potential was measured with a pressure chamber (Soil Moisture Equipment) and leaf elongation rate of the sixth leaf was monitored every 15 min with rotational displacement transducers (601-1045 Full 360° Smart Position Sensor; Spectrol Electronics), following the protocol of Sadok et al. (2007). At time 0, plants were rewatered until retention capacity and placed in dark conditions at a VPD of 0.8 kPa, which virtually stopped transpiration. Measurements of leaf elongation rate and leaf water potential were carried out in the following 18 h.

Plant Measurements in Greenhouse Experiments

All measurements were carried out in plants at the six- or seven-leaf stage. Leaf water potential of nonexpanding leaves was measured at midday with a pressure chamber (experiments 1–3, days without clouds between 11 AM and 1 PM). Stomatal conductance was measured with a diffusion porometer (AP4; Delta-T Devices) calibrated every 30 min (same experiments and conditions as for leaf water potential measurements). Only nonexpanding leaves receiving full light were measured. Because values differed slightly between experiments (from 120 to 180 mmol m^{-2} s^{-1}), each value was normalized by the mean value of the well-watered WT plants of the corresponding day.

Plant transpiration was estimated from the weight loss of each column every 15 min (Table II, experiment 3). Direct evaporation from the soil was estimated by measuring the weight loss of soil columns without plants watered at the same time as other columns. Plant transpiration was divided by leaf area, measured nondestructively every third day by measuring the length and width of each leaf (Chenu et al., 2008).

Root area was measured in one experiment (Table II, experiment 3) at the six-leaf stage. Roots were first cleaned with water, and then primary and secondary roots were separated. Three samples (5–10 cm length) of each root type of each plant were scanned and area was determined with an image analyzer. All samples plus the whole root systems were dried at 85°C for 3 d and weighed. The ratio of area to weight was determined for each root type and each genotype, so the area of each root system was calculated from the biomass of each root type and the ratio of area to weight of the corresponding sample.

Pressure-Volume Curves and ABA Measurements

Water-release curves of plants at the six-leaf stage were obtained in three to five plants per line (experiment 4). Leaves of well-watered plants, grown in the dark for 12 h, were cut, weighed (fresh weight), and placed into a pressure chamber. The pressure was increased in five steps of 0.5 MPa for 15 min each, during which the sap exudate was collected in a tube. When the sap flow stopped, the water potential was determined and the accumulated sap flow was estimated by weighing the tube. It was determined that sap evaporation did not exceed 10% of the total sap collected in each leaf. At the end of the measurements, the leaf was dried at 85°C for 3 d and weighed. The relative water content was calculated as the difference between weight and dry weight divided by the difference between fresh weight and dry weight.

The concentration of ABA was measured in sap samples obtained by pressurizing leaves in the pressure chamber in the early morning (experiments 1–3). Sap samples were then stored at −80°C until analysis. ABA concentration was then measured in crude samples of xylem sap by radioimmunoassay (Quarrie et al., 1988) as described previously (Barrieu and Simonneau, 2000).

RNA Extraction and Quantitative RT-PCR (Experiment 8)

RNA extraction was carried out as described by Hachez et al. (2006). Briefly, total RNA was extracted from thoroughly ground frozen root sections using an RNeasy Plant Extraction Minikit (Qiagen). DNase I digestion was performed on a column during RNA extraction according to the manufacturer's recommendations. cDNA synthesis and real-time PCR were then performed as described by Hachez et al. (2006). Results were normalized using two maize internal control genes, *α-tubulin* (gi: 450292; Hachez et al., 2006) and *actin* (gi:168403; forward primer, 5′-TTGGGTCAGAAAGGTTCAGG-3′; reverse primer, 5′-GCACTTCATGTGGACAATGC-3′). ZmPIP primers were those used by Hachez et al. (2006) targeting a 100-bp-long sequence from the 3′ untranslated region. NCED mRNA levels were assessed using 20-bp-long specific primers (forward primer, 5′-ATCAAGAGGCCGTACCTCAA-3′; reverse primer, 5′-GCATCTCCTGGAGCTTGAAC-3′). PCR efficiency of the NCED primers was checked and found to be appropriate.

Protein Extraction and Analysis

Measurements were carried out on plants grown hydroponically until the six-leaf stage (experiment 5) and subjected to a 72-h water stress obtained with PEG (−0.4 MPa; PEG8000, 150 g L^{-1}). Root tips (4 cm) and the leaf elongation zone (6 cm) were collected during early morning, immediately placed in a tube immersed in liquid nitrogen, and stored at −80°C. To prepare the microsomal fraction, 1 g of tissue was ground in 1.5 mL of solution (250 mM sorbitol, 50 mM Tris-HCl [pH 8], and 2 mM EDTA) containing 0.6% polyvinylpyrrolidone, 0.5 mM dithiothreitol, and protease inhibitors (1 μg mL^{-1} each of leupeptin, aprotinin, antipain, chymostatin, and pepstatin [Sigma]). All subsequent steps were performed at 4°C as described (Hachez et al., 2006). Fifteen micrograms of crude microsomal membranes was solubilized for 15 min at 60°C in a buffer (80 mM Tris-HCl, 2% SDS, 10% glycerol, 0.005% bromphenol blue, and 1% dithiothreitol), and the proteins were separated by SDS-PAGE on a 12% polyacrylamide gel. After electrophoresis, the gel was incubated for 5 min in semidry buffer (48 mM Tris, 39 mM Gly, 20% methanol, and 0.0375% SDS) before semidry transfer to a polyvinylidene difluoride (Millipore) membrane for 40 min at 23 V. Western-blot analysis was performed on the polyvinylidene difluoride membrane using antiserum raised against the N-terminal peptides of ZmPIP1;2, ZmPIP2;1, ZmPIP2;5, and ZmPIP2;6 (Chaumont et al., 2001). The antiserum raised against ZmPIP2;1 also recognized ZmPIP2;2 (Hachez et al., 2006). The dilutions used were 1:1,000 for the ZmPIP1;2, ZmPIP2;5, and ZmPIP2;6 antiserum and 1:3,500 for the ZmPIP2;1/2;2 antiserum. Detection and protein quantification were carried out using a Kodak 4000R image station and the associated software. Three different exposure times were used per experiment for accurate protein quantification.

Measurement of Lp_r in Nutrient Solution

Measurements were carried out from 10 AM to 1 PM, while Lp_r was maximum (experiments 6 and 7). The free exudation rate of the excised seminal root system was measured by collecting exuded sap with a micropipette and weighing it in microtubes. The osmotic potentials of the sap and of the nutrient solution were measured with a vapor pressure osmometer (Vapro 5520; Wescor).

A hydrostatically driven xylem sap flow was triggered in excised root systems by applying a vacuum-induced tension (Freundl et al., 1998). The seminal root system was excised by sectioning the mesocotyl and then fixed tightly to a silicon tube using low-viscosity dental paste (President Light; Coltene Whaledent). The silicon tube was connected to a vacuum port equipped with a tension gauge. A two-valve system driven by the data logger allowed automatic control of the tension applied to the seminal roots. After 30 min, needed to stabilize the exudation rate, the water flux was

measured every 10 min. The suction force applied to the root system was varied every 10 min in a standardized way (0, −0.02, −0.04, −0.06, −0.06, −0.04, −0.02, and 0 MPa). The water flow across the root system was measured with a water trap made of a 2-mL tube filled with dry cotton and inserted onto the tubing between the roots and the vacuum port. Water flow was measured by weighing the sap absorbed by the cotton that was renewed every 10 min. H_2O_2 treatment (2 mM) was applied to the root system after 40 min, and the depressurization protocol was then applied in the same way. At the end of each experiment, the root system was scanned and root area (A) was determined with an image analyzer.

The Lp_r under an osmotic gradient (Lp_{os}) was calculated as follows:

$$Lp_{os} = J(\pi_{sap} - \pi_{sol})^{-1} \times A^{-1} \quad (1)$$

where J is the water flux through the root system without depressurization, π_{sap} and π_{sol} are the osmotic potentials of the sampled sap and of the nutrient solution, respectively, and A is the area of the root system. Lp_r under a hydrostatic gradient (Lp_h) was calculated from the slope of the regression between water flow and the suction applied to the root system (dJ/dP):

$$Lp_h = (dJ/dP) \times A^{-1} \quad (2)$$

Model of Water Transfer

The model of stomatal control, biosynthesis of ABA, and water transfer is that of Tardieu and Davies (1993). This model calculates stomatal conductance, $[ABA]_{xyl}$, water flux, root and the water potentials in transpiration sites from soil water potential, light intensity, and air VPD. The parameters used in calculations were those of the original paper, except for (1) the parameter that relates ABA biosynthesis to root water potential, which was calibrated for WT, AS, and S lines according to the measured $[ABA]_{xyl}$, and (2) the root hydraulic conductance, which was calculated from the hydraulic conductivities presented in Figure 5 and the measured root area presented in Figure 2 (Table I).

Changes in the model were added to allow simulation of the water potential of leaf cells. The water potential at leaf evaporating sites (Ψ_{evap}) was calculated from the xylem water potential (Ψ_{xyl}), the water flux (J), and the conductance to the flux from xylem to leaves ($g_{x\text{-}s}$):

$$\Psi_{evap} = \Psi_{xyl} - J/g_{x\text{-}s} \quad (3)$$

This conductance was estimated by measuring leaf and xylem water potentials of maize plants at the same stage (Table I).

Leaves presented a capacitance that was calculated from the pressure-volume curve presented in Figure 8 and the estimate of the leaf volume. They were a sink for water when their potential was lower than that of the evaporating sites and a source otherwise. The water flux corresponding to leaf growth during the considered 6 h of the simulation was negligible. Therefore, we solved the differential equation for calculating the cell water potential (Ψ_{cel}) and the water flux from the xylem to the leaf cells (J_{xc}):

$$J_{xc} = dV_{cell}/dt = g_{x\text{-}l}(\Psi_{xyl} - \Psi_{cel}) \quad (4)$$

where $g_{x\text{-}l}$ is the conductance of the pathway from xylem to leaf cells. At each time i, the flux through roots and xylem was the sum of the transpiration flux (J) and of the water flux from the xylem to the leaf cells (J_{xc}), so

$$\Psi_{cel} = \Psi_{soil}(i) - R_{sp}(i \times (J + J_{xc})) - R_r \times (J + J_{xc}) - (J + J_{xc})/g_{x\text{-}l} \quad (5)$$

where R_{sp} is the resistance to water flow in the soil, calculated as by Tardieu and Davies (1993), R_r is the resistance to water flux in the root system, calculated from Lp_r measured experimentally and root area (Table I), and $g_{x\text{-}l}$ is as in Equation 4 (Table I).

A first calculation of J_{xc} was derived from Equations 4 and 5:

$$J_{xc} = (g_{x\text{-}l} \times (-\Psi_{cel} + \Psi_{soil} - R_{sp} \times J - R_r \times J - J/g_{x\text{-}l}))/ (1 + L_p \times R_{sp} + L_p \times R_r + L_p/g_{x\text{-}l}) \quad (6)$$

A second expression of J_{xc} was obtained from the relationship between V_{cell} and Ψ_{cel}:

$$V_{cell} = V_{res} + (V_{sat} - V_{res}) \times (1/(1 + (\alpha \times (-\Psi_{cel}))^n))^{(1 - 1/n)} \quad (7)$$

where V_{sat} is the leaf volume at saturation (early morning), V_{res} is the residual volume at the water potential at the end of the experiment, and α and n are the parameters of a Van Genuchten equation fitted on the pressure volume curve. J_{xc} was calculated as the difference in V_{cell} between two different times for the optimization process of resolution of the differential equation. L_p was the only fitted parameter of the model. The elastic modulus of leaves was common to the three lines because the curves relating turgor to volume were indistinguishable in AS, S, and WT lines (Fig. 8).

Supplemental Data

The following materials are available in the online version of this article.

Supplemental Figure S1. Expression levels of the *NCED/VP14* gene in roots in AS (AS5) and S plants relatively to their value in WT plants.

ACKNOWLEDGMENTS

We thank P. Hamard for the development of the technique for measuring Lp_r and Gaelle Rolland for measurements of ABA concentration.

Received October 1, 2008; accepted February 6, 2009; published February 11, 2009.

LITERATURE CITED

Aroca R, Ferrante A, Vernieri P, Chrispeels MJ (2006) Drought, abscisic acid and transpiration rate effects on the regulation of PIP aquaporin gene expression and abundance in *Phaseolus vulgaris* plants. Ann Bot (Lond) **98:** 1301–1310

Aroca R, Vernieri P, Irigoyen JJ, Sànchez-Diaz M, Tognoni F, Pardossi A (2003) Involvement of abscisic acid in leaf and root of maize (*Zea mays* L.) in avoiding chilling-induced water stress. Plant Sci **165:** 671–679

Bacon MA, Wilkinson S, Davies WJ (1998) pH-regulated leaf cell expansion in droughted plants is abscisic acid dependent. Plant Physiol **118:** 1507–1515

Barrieu P, Simonneau T (2000) The monoclonal antibody MAC252 does not react with the (−) enantiomer of abscisic acid. J Exp Bot **51:** 305–307

Barrowclough DE, Peterson CA, Steudle E (2000) Radial hydraulic conductivity along developing onion roots. J Exp Bot **51:** 547–557

Beaudette PC, Chlup M, Yee J, Emery RJN (2007) Relationships of root conductivity and aquaporin gene expression in *Pisum sativum*: diurnal patterns and the response to $HgCl_2$ and ABA. J Exp Bot **58:** 1291–1300

Ben Haj Salah H, Tardieu F (1997) Control of leaf expansion rate of droughted maize plants under fluctuating evaporative demand: a superposition of hydraulic and chemical messages? Plant Physiol **114:** 893–900

Benjamini Y, Hochberg Y (1995) Controlling the false discovery rate: a practical and powerful approach to multiple testing. J R Stat Soc Ser B Stat Methodol **57:** 289–300

Borel C, Frey A, Marion-Poll A, Tardieu F, Simonneau T (2001) Does engineering abscisic acid biosynthesis in *Nicotiana plumbaginifolia* modify stomatal response to drought? Plant Cell Environ **24:** 477–489

Boursiac Y, Boudet J, Postaire O, Luu DT, Tournaire-Roux C, Maurel C (2008) Stimulus-induced downregulation of root water transport involves reactive oxygen species-activated cell signalling and plasma membrane intrinsic protein internalization. Plant J **56:** 207–218

Chaumont F, Barrieu F, Jung R, Chrispeels MJ (2000) Plasma membrane intrinsic proteins from maize cluster in two sequence subgroups with differential aquaporin activity. Plant Physiol **122:** 1025–1034

Chaumont F, Barrieu F, Wojcik E, Chrispeels MJ, Jung R (2001) Aquaporins constitute a large and highly divergent protein family in maize. Plant Physiol **125:** 1206–1215

Chenu K, Chapman SC, Hammer GL, McLean G, Ben Haj Salah H, Tardieu F (2008) Short-term responses of leaf growth rate to water deficit scale up to whole-plant and crop levels: an integrated modelling approach in maize. Plant Cell Environ **31:** 378–391

Christmann A, Weiler EW, Steudle E, Grill E (2007) A hydraulic signal in root-to-shoot signalling of water shortage. Plant J **52:** 167–174

Dewar RC (2002) The Ball-Berry-Leuning and Tardieu-Davies stomatal

models: synthesis and extension within a spatially aggregated picture of guard cell function. Plant Cell Environ **25:** 1383–1398

Endo A, Sawada Y, Takahashi H, Okamoto M, Ikegami K, Koiwai H, Seo M, Toyomasu T, Mitsuhashi W, Shinozaki K, et al (2008) Drought induction of Arabidopsis 9-cis-epoxycarotenoid dioxygenase occurs in vascular parenchyma cells. Plant Physiol **147:** 1984–1993

Fetter K, Van Wilder V, Moshelion M, Chaumont F (2004) Interactions between plasma membrane aquaporins modulate their water channel activity. Plant Cell **16:** 215–228

Freundl E, Steudle E, Hartung W (1998) Water uptake by roots of maize and sunflower affects the radial transport of abscisic acid and its concentration in the xylem. Planta **207:** 8–19

Gordon-Kamm WJ, Spencer TM, Mangano ML, Adams TR, Daines RJ, Start WG, O'Brien JV, Chambers SA, Adams WR Jr, Willetts NG, et al (1990) Transformation of maize cells and regeneration of fertile transgenic plants. Plant Cell **2:** 603–618

Gutschick VP, Simonneau T (2002) Modelling stomatal conductance of field-grown sunflower under varying soil water content and leaf environment: comparison of three models of stomatal response to leaf environment and coupling with an abscisic acid-based model of stomatal response to soil drying. Plant Cell Environ **25:** 1423–1434

Hachez C, Heinen RB, Draye X, Chaumont F (2008) The expression pattern of plasma membrane aquaporins in maize leaf highlights their role in hydraulic regulation. Plant Mol Biol **68:** 337–353

Hachez C, Moshelion M, Zelazny E, Cavez D, Chaumont F (2006) Localization and quantification of plasma membrane aquaporin expression in maize primary root: a clue to understanding their role as cellular plumbers. Plant Mol Biol **62:** 305–323

Hose E, Steudle E, Hartung W (2000) Abscisic acid and hydraulic conductivity of maize roots: a study using cell- and root-pressure probes. Planta **211:** 874–882

Ishida Y, Saito H, Ohta S, Hiei Y, Komari T, Kumashiro T (1996) High efficiency transformation of maize (*Zea mays* L.) mediated by *Agrobacterium tumefaciens*. Nat Biotechnol **14:** 745–750

Jang JY, Kim DG, Kim YO, Kim JS, Kang H (2004) An expression analysis of a gene family encoding plasma membrane aquaporins in response to abiotic stresses in *Arabidopsis thaliana*. Plant Mol Biol **54:** 713–725

Kaldenhoff R, Kölling A, Richter G (1996) Regulation of the *Arabidopsis thaliana* aquaporin gene AthH2 (*PIP1b*). J Photochem Photobiol B **36:** 351–354

Kaldenhoff R, Ribas-Carbo M, Flexas J, Lovisolo C, Heckwolf M, Uehlein U (2008) Aquaporins and plant water balance. Plant Cell Environ **31:** 658–666

Lee SH, Chung GC, Steudle E (2005) Low temperature and mechanical stresses differently gate aquaporins of root cortical cells of chilling-sensitive cucumber and -resistant figleaf gourd. Plant Cell Environ **28:** 1191–1202

Lian HL, Yu X, Ye Q, Ding XS, Kitagawa Y, Kwak SS, Su WA, Tang ZC (2004) The role of aquaporin RWC3 in drought avoidance in rice. Plant Cell Physiol **45:** 481–489

Lo Gullo MA, Nardini A, Salleo S, Tyree MT (1998) Changes in root hydraulic conductance (KR) of *Olea oleaster* seedlings following drought stress and irrigation. New Phytol **140:** 25–31

Mariaux JB, Bockel C, Salamini F, Bartels D (1998) Desiccation- and abscisic acid-responsive genes encoding major intrinsic proteins (MIPs) from the resurrection plant *Craterostigma plantagineum*. Plant Mol Biol **38:** 1089–1099

Martre P, Morillon R, Barrieu F, North GB, Nobel PS, Chrispeels MJ (2002) Plasma membrane aquaporins play a significant role during recovery from water deficit. Plant Physiol **130:** 2101–2110

Martre P, North GB, Nobel PS (2001) Hydraulic conductance and mercury-sensitive water transport for roots of *Opuntia acanthocarpa* in relation to soil drying and rewetting. Plant Physiol **126:** 352–362

Maurel C, Verdoucq L, Luu DT, Santoni V (2008) Plant aquaporins: membrane channels with multiple integrated functions. Annu Rev Plant Biol **59:** 595–624

Morillon R, Chrispeels MJ (2001) The role of ABA and the transpiration stream in the regulation of the osmotic water permeability of leaf cells. Proc Natl Acad Sci USA **98:** 14138–14143

North GB, Martre P, Nobel PS (2004) Aquaporins account for variations in hydraulic conductance for metabolically active root regions of *Agave deserti* in wet, dry, and rewetted soil. Plant Cell Environ **27:** 219–228

Qin X, Zeevaart JAD (1999) The 9-cis-epoxycarotenoid cleavage reaction is the key regulatory step of abscisic acid biosynthesis in water-stressed bean. Proc Natl Acad Sci USA **96:** 15354–15361

Quarrie S, Whitford P, Appleford N, Wang T, Cook S, Henson I, Loveys B (1988) A monoclonal antibody to (S)- abscisic acid: its characterization and use in a radioimmunoassay for measuring abscisic acid in crude extracts of cereal and lupin leaves. Planta **173:** 330–339

Quintero J, Fournier J, Benlloch M (1999) Water transport in sunflower root systems: effects of ABA, Ca^{2+} status and $HgCl_2$. J Exp Bot **50:** 1607–1612

Sadok W, Naudin P, Boussuge B, Muller B, Welcker C, Tardieu F (2007) Leaf growth rate per unit thermal time follows QTL-dependent daily patterns in hundreds of maize lines under naturally fluctuating conditions. Plant Cell Environ **30:** 135–146

Sansberro PA, Mroginski LA, Bottini R (2004) Foliar sprays with ABA promote growth of *Ilex paraguariensis* by alleviating diurnal water stress. Plant Growth Regul **42:** 105–111

Sauter A, Abrams S, Hartung W (2002) Structural requirements of abscisic acid (ABA) and its impact on water flow during radial transport of ABA analogues through maize roots. J Plant Growth Regul **21:** 50–59

Schraut D, Heilmeier H, Hartung W (2005) Radial transport of water and abscisic acid (ABA) in roots of *Zea mays* under conditions of nutrient deficiency. J Exp Bot **56:** 879–886

Sharp RE (2002) Interaction with ethylene: changing views on the role of abscisic acid in root and shoot growth responses to water stress. Plant Cell Environ **25:** 211–222

Shinozaki K, Yamaguchi-Shinozaki K, Mizoguchi T, Urao T, Katagiri T, Nakashima K, Abe H, Ichimura K, Liu Q, Nanjyo T, et al (1998) Molecular responses to water stress in *Arabidopsis thaliana*. J Plant Res **111:** 345–351

Steudle E (2000) Water uptake by plant roots: an integration of views. Plant Soil **226:** 45–56

Tan BC, Schwartz SH, Zeevaart JAD, McCarty DR (1997) Genetic control of abscisic acid biosynthesis in maize. Proc Natl Acad Sci USA **94:** 12235–12240

Tardieu F, Davies WJ (1993) Integration of hydraulic and chemical signalling in the control of stomatal conductance and water status of droughted plants. Plant Cell Environ **16:** 341–349

Thompson AJ, Andrews J, Mulholland BJ, McKee JMT, Hilton HW, Horridge JS, Farquhar GD, Smeeton RC, Smillie IRA, Black CR, et al (2007a) Overproduction of abscisic acid in tomato increases transpiration efficiency and root hydraulic conductivity and influences leaf expansion. Plant Physiol **143:** 1905–1917

Thompson AJ, Jackson AC, Symonds RC, Mulholland BJ, Dadswell AR, Blake PS, Burbidge A, Taylor IB (2000) Ectopic expression of a tomato 9-cis-epoxycarotenoid dioxygenase gene causes over-production of abscisic acid. Plant J **23:** 363–374

Thompson AJ, Mulholland BJ, Jackson AC, McKee JMT, Hilton HW, Symonds RC, Sonneveld T, Burbidge A, Stevenson P, Taylor IB (2007b) Regulation and manipulation of ABA biosynthesis in roots. Plant Cell Environ **30:** 67–78

Tournaire-Roux C, Sutka M, Javot H, Gout E, Gerbeau P, Luu DT, Bligny R, Maurel C (2003) Cytosolic pH regulates root water transport during anoxic stress through gating of aquaporins. Nature **425:** 393–397

Tyerman SD, Niemietz CM, Bramley H (2002) Plant aquaporins: multifunctional water and solute channels with expanding roles. Plant Cell Environ **25:** 173–194

Vandeleur RK, Mayo G, Shelden MC, Gilliham M, Kaiser BN, Tyerman SD (2009) The role of plasma membrane intrinsic protein aquaporins in water transport through roots: diurnal and drought stress responses reveal different strategies between isohydric and anisohydric cultivars of grapevine. Plant Physiol **149:** 445–460

Voisin AS, Reidy B, Parent B, Rolland G, Redondo E, Gerentes D, Tardieu F, Muller B (2006) Are ABA, ethylene or their interaction involved in the response of leaf growth to soil water deficit? An analysis using naturally occurring variation or genetic transformation of ABA production in maize. Plant Cell Environ **29:** 1829–1840

Wan X, Steudle E, Hartung W (2004) Gating of water channels (aquaporins) in cortical cells of young corn roots by mechanical stimuli (pressure pulses): effects of ABA and of $HgCl_2$. J Exp Bot **55:** 411–422

Wan X, Zwiazek JJ (1999) Mercuric chloride effects on root water transport in aspen seedlings. Plant Physiol **121:** 939–946

Wan X, Zwiazek JJ (2001) Root water flow and leaf stomatal conductance in

aspen (*Populus tremuloides*) seedlings treated with abscisic acid. Planta **213:** 741–747

Ye Q, Steudle E (2006) Oxidative gating of water channels (aquaporins) in corn roots. Plant Cell Environ **29:** 459–470

Zelazny E, Borst JW, Muylaert M, Batoko H, Hemminga MA, Chaumont F (2007) FRET imaging in living maize cells reveals that plasma membrane aquaporins interact to regulate their subcellular localization. Proc Natl Acad Sci USA **104:** 12359–12364

Zhang J, Davies WJ (1990a) Changes in the concentration of ABA in xylem sap as a function of changing soil water status can account for changes in leaf conductance. Plant Cell Environ **13:** 277–285

Zhang J, Davies WJ (1990b) Does ABA in the xylem control the rate of leaf growth in soil-dried maize and sunflower plants? J Exp Bot **41:** 1125–1132

Zhang WH, Tyerman SD (1999) Inhibition of water channels by $HgCl_2$ in intact wheat root cells. Plant Physiol **120:** 849–858

Zhu C, Schraut D, Hartung W, Schaffner AR (2005) Differential responses of maize MIP genes to salt stress and ABA. J Exp Bot **56:** 2971–2981